DOI: 10.1002/ejic.201000081

Structural and Magnetic Studies of New Ni^{II}–Ln^{III} Complexes

Jean-Pierre Costes*[a,b] and Laure Vendier[a,b]

Keywords: Coordination Chemistry / Nickel / Lanthanides / Structure elucidation / Magnetic properties

The synthesis, structure determination and magnetic studies of dinuclear Ni^{II}–Ln^{III} complexes (Ln = Y, La, Pr, Gd) involving *ortho*-vanillin as the main ligand are described. Structural studies demonstrate that two types of complexes can be obtained with hexacoordinate Ni ions in slightly deformed octahedral environments and nine- or ten-coordinate lanthanide ions. The Ni and Gd ions are linked by two phenoxo bridges in one complex and two phenoxo bridges and one nitrato bridge in the other. A ferromagnetic interaction operates in the Ni–Gd complex, with a *D* zero field splitting term for the nickel ion, as in the Ni–La and Ni–Y complexes where these *D* terms are the only active magnetic terms. Among the factors responsible for the different structures are ionic radii of the Ln ions, solvent and configuration change of the starting nickel complex; the role of solvent seems to be preponderant. The weak value of the ferromagnetic Ni–Gd interaction can be explained by the flexibility and the departure from planarity of the two independent *ortho*-vanillin ligands.

Introduction

Schiff base ligands have been used to assemble hetero di- or heterotrinuclear 3d–4f complexes.[1–3] Many of these ligands have been prepared with *ortho*-vanillin (ovanH), which yields compartmental Schiff base ligands with two different coordination sites; 3d ions have a marked affinity for the inner N_2O_2 site, whereas 4f ions prefer the outer, larger O_2O_2 coordination site. In view of these observations, we decided to use *ortho*-vanillin as the main ligand in our study. The first examples of such 3d–4f compounds were Cu–Ln[4] and Co–Ln[5] complexes. Such a synthetic method has been recently used to obtain interesting Cu–Tb complexes that behave as single molecule magnets.[6] *ortho*-Vanillin can also yield trinuclear Ln complexes (Ln = Gd, Dy)[7–8] and can be used as a starting material to isolate tetranuclear Dy_4 complexes[9–10] with large anisotropy barriers. In the present study, we introduce the synthesis of the first dinuclear Ni^{II}–Ln complexes prepared from *ortho*-vanillin, the structural determinations of two of these compounds and an investigation of the magnetic properties of the Ni–La, Ni–Pr, Ni–Gd and Ni–Y complexes.

Results and Discussion

ortho-Vanillin reacts with nickel acetate to yield a green precipitate characterized as $(ovan)_2Ni(H_2O)_2$. The two deprotonated ovan ligands are in a *trans* arrangement, as in the corresponding salicylaldehydato nickel complex.[11] The coordination of a Ln ion necessitates the change from *trans* to *cis* conformation of these ligands, as previously observed with alkaline ions.[12] Addition of lanthanum or praseodymium nitrate to the nickel starting complex in acetone gives the Ni–Ln complexes,[13] $[(H_2O)_2Ni(ovan)_2Ln(NO_3)_3]$ (Ln = La, Pr). As we could not obtain crystals with gadolinium under these experimental conditions, the reaction was performed in methanol. The resulting Gd complex differs from the previous complexes prepared in acetone by its formulation. The analytical data indicate that a nitrato anion has been replaced by a third ovan ligand. Crystals suitable for XRD determination were obtained for the product with yttrium, and the isomorphism of the corresponding gadolinium complex was checked by X-ray powder diffraction.

Structure Determination

The nickel–praseodymium complex **2** crystallizes in the monoclinic space group $P2_1/c$ with $Z = 4$. The crystallographic data for **2** are collated in Table 1, and selected bond lengths and angles are given in the caption of Figure 1. The structure determination of complex **2** gives evidence for the existence of a dinuclear Ni–Pr complex molecule, as shown in Figure 1. This molecule may be formulated as $[(H_2O)_2Ni(ovan)_2Pr(NO_3)_3]$. As expected, the nitrato anions are chelated to the Pr centre, which is ten-coordinate to the two phenoxo and the two methoxy oxygen atoms of the two deprotonated ovan ligands and to the six oxygen atoms of the three chelating nitrato anions. The nickel ion is six-coordinate to the phenoxo and aldehyde oxygen atoms of the two deprotonated ovan ligands and to the two oxygen atoms of the axial water ligands. The central NiO_2Pr core of the molecule is practically planar, the dihedral angle be-

[a] CNRS, LCC (Laboratoire de Chimie de Coordination), 205, route de Narbonne, 31077 Toulouse, France
E-mail: costes@lcc-toulouse.fr
[b] Université de Toulouse, UPS, INPT, LCC, 31077 Toulouse, France

Supporting information for this article is available on the WWW under http://dx.doi.org/10.1002/ejic.201000081.

tween the NiO1O2 and PrO1O2 planes is 1.3(1)° and the Ni···Pr separation is 3.5614(4) Å. The deviation of the nickel ion from the mean O_2O_2 plane of the ovan ligands is only 0.0370(3) Å. There are two intramolecular hydrogen bonds involving the water molecules and the nearest nitrato oxygen atom linked to the Pr ion, yielding two S(6) graph sets.[14] The two nitrato ligands chelated in the axial position are further involved in intermolecular hydrogen bonds by their non-coordinated oxygen atoms. These inter- and intramolecular hydrogen bonds form rings that position the Ni–Pr complexes in a head-to-tail arrangement. Furthermore, the different orientations of these nitrato ligands imply that the same nitrato ligands of two neighbouring NiPr units are involved in a ring, so that there are two different $R_4^4(12)$ graph sets[14] that give 1D chains of alternate Ni–Pr units (Figure S2). One of these rings has supplementary contacts with the nitrato oxygen atom of the third NO_3 ligand not involved in Pr coordination (O17) and the NO_3 oxygen atom O11 involved in the intermolecular hydrogen bond, thus giving 2D arrays. Nevertheless, these NiPr units are isolated from each other, with intermolecular Ni···Ni, Pr···Pr and Ni···Pr distances all larger than 7.3 Å. The coordination geometry around each Ni centre was analyzed with a continuous shape measure carried out with the SHAPE program,[15] which confirms that Ni is not far from perfect octahedral geometry [$S(O_h) = 0.63$] (the S coefficient varies from zero for an ideal octahedron to one hundred).

Table 1. Crystallographic data for complexes **2** and **3**.

	2	**3**
Formula	$C_{16}H_{18}N_3NiO_{17}Pr$	$C_{24}H_{25}N_2NiO_{17}Y$
F_w	723.95	761.08
Space group	$P2_1/c$ (No. 14)	$P2_1/n$ (No. 14)
a (Å)	9.4451(8)	11.3830(8)
b (Å)	18.3377(10)	15.5370(7)
c (Å)	14.5668(9)	16.4140(6)
α (°)	90	90
β (°)	106.340(7)	91.749(5)
γ (°)	90	90
V (Å^3)	2421.1(3)	2901.6(3)
Z	4	4
$\rho_{calcd.}$ (g cm^{-3})	1.986	1.742
λ (Å)	0.71073	0.71073
T (K)	293(2)	180(2)
μ(Mo-K_α) (mm^{-1})	2.854	2.723
R[a] obsd., all	0.0211, 0.0344	0.0241, 0.0345
Rw[b] obsd., all	0.0491, 0.591	0.052, 0.0556

[a] $R = \Sigma||F_o| - |F_c||/\Sigma|F_o|$. [b] $wR_2 = [\Sigma w(|F_o^2| - |F_c^2|)^2/\Sigma w|F_o^2|^2]^{1/2}$.

The nickel–yttrium complex **3** mainly differs from **2** by the departure from planarity of the two ovan ligands defining the nickel equatorial plane depicted in Figure 2. One water molecule is axially linked to nickel; two nitrato ligands and a chelating *ortho*-vanillinato ligand are coordinated to the Y centre in place of a NO_3 ligand, completing the metal coordination spheres. The Y ion is nine-coordinate. The second water molecule, present in **2**, is replaced by the oxygen atom of a bridging nitrato ligand. The second nitrato ligand chelates the Y ion, so that **3** is formulated as $[(H_2O)Ni(ovan)_2(\mu\text{-}NO_3)Y(ovan)(NO_3)_2]H_2O$. The bridging and chelating NO_3 ligands are located on the same side of

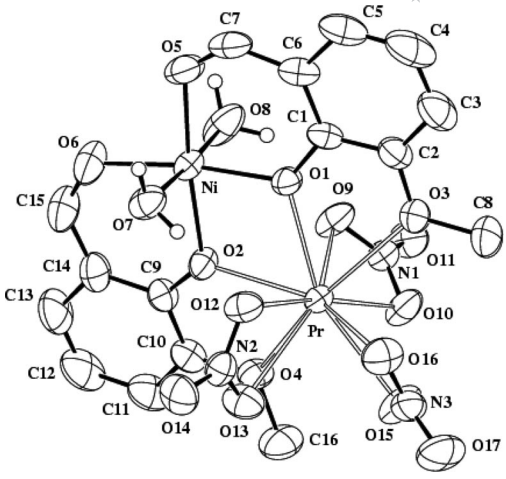

Figure 1. Plot of **2** with ellipsoids drawn at the 50% probability level and with atom numbering. Hydrogen atoms, except those of the water molecules, have been omitted for clarity. Selected bond lengths [Å] and angles [°]: Ni–O1 2.0052(18), Ni–O2 2.0067(18), Ni–O5 2.009(2), Ni–O6 2.011(2), Ni–O8 2.074(2), Ni–O7 2.078(2), Pr–O1 2.4086(17), Pr–O2 2.4037(17), Pr–O3 2.612(2), Pr–O4 2.5806(18), Pr–O9 2.600(2), Pr–O10 2.561(2), Pr–O12 2.598(2), Pr–O13 2.631(2), Pr–O15 2.554(2), Pr–O16 2.600(2), O2–Pr–O1 65.05(6), O1–Ni–O2 80.33(7), Ni–O1–Pr 107.23(7), Ni–O2–Pr 107.37(7).

the equatorial $Ni(ovan)_2Y$ part of the molecule, while the water and *ortho*-vanillinato ligands are positioned on the other side. The Ni ion does not really depart from the mean equatorial O_2O_2 plane of the two ovan ligands [0.0106(2) Å] and the NiO_2Y core is planar, the dihedral angle between the NiO1O2 and YO1O2 planes is 0.8(1)°, and the Ni···Y distance of 3.3244(3) Å. On the contrary, the angles be-

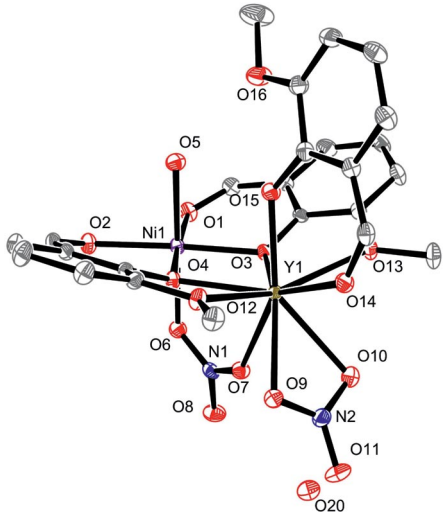

Figure 2. Plot of **3** with ellipsoids drawn at the 30% probability level and with atom numbering. Hydrogen atoms have been omitted for clarity. Selected bond lengths [Å] and angles [°]: Ni–O1 2.0209(14), Ni–O2 2.0210(14), Ni–O3 1.9919(13), Ni–O4 2.0027(13), Ni–O5 2.0433(15), Ni–O6 2.0838(14), Y–O3 2.2864(13), Y–O4 2.2832(13), Y–O7 2.5423(14), Y–O9 2.4358(14), Y–O10 2.4500(14), Y–O12 2.6035(14), Y–O13 2.5418(14), Y–O14 2.3143(14), Y–O15 2.2222(14), O3–Ni1–O4 84.61(5), O4–Y1–O3 72.09(5), Ni1–O3–Y1 101.76(5), Ni1–O4–Y1 101.53(5)°.

tween the O_2O_2 plane and each ovan ligand, which are 25.3(1) and 21.7(1)°, respectively, introduce a larger deformation of the equatorial plane than that in **2**. The water molecule linked to nickel is involved in a weak intramolecular hydrogen bond with the methoxy and phenoxo oxygen atoms of the ovan ligand chelated to Y [S(5) graph set][14] and in a stronger hydrogen bond with the free water molecule, which is also hydrogen bonded to the outer oxygen atom of the nitrato bridging ligand. This C(4) graph set[14] defines an infinite 1D chain of Ni–Y units (Figure S3), with Ni···Y interchain distances of 6.604(2) Å and intra chain Ni···Y distances larger than 8.5 Å. The SHAPE program[15] indicates that the Ni ion is not far from a perfect octahedral geometry [$S(O_h)$ = 0.14]. Although crystals of complex **4** could not be used for a structure determination, the X-ray powder diffraction data of **4** allowed us to find the parameters of the unit cell by an ab initio search (Figure S1). This result clearly demonstrates that complexes **3** and **4** are isomorphous.

Magnetic Properties

The $\chi_M T$ product shown in Figure 3 for **4** is 9.6 $cm^3 mol^{-1}$ K at 300 K. From 300 to 40 K, a slight increase to 10.0 $cm^3 mol^{-1}$ K is observed, followed by a sharp increase from 40 to 2 K where it is 12.5 $cm^3 mol^{-1}$ K. The $\chi_M T$ value at room temperature is slightly larger than that expected for one isolated Ni and one Gd ion (8.9 $cm^3 mol^{-1}$ K) with g = 2, but corresponds to that expected for a g value of 2.07 (9.5 $cm^3 mol^{-1}$ K).

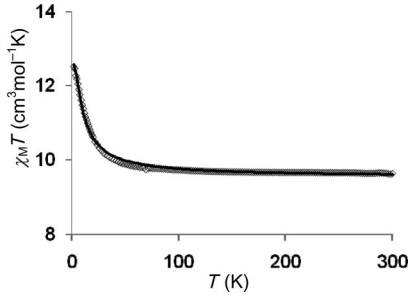

Figure 3. Temperature dependence of the $\chi_M T$ product for **4**. The solid line corresponds to J_{NiGd} = 1.36 cm^{-1}, g = 2.07, D_{Ni} = 4.6 cm^{-1}, R = 2.0 10^{-5}.

The experimental data indicate the occurrence of an overall ferromagnetic interaction in **4**. The magnetic susceptibility has been computed by exact calculation of the energy levels associated with the spin Hamiltonian $H = -J_{NiGd}(S_{Ni} \cdot S_{Gd})$ through diagonalization of the full energy matrix. The best fit (Figure S4) yields the following data, J_{NiGd} = 1.28 cm^{-1}, g = 2.07 with a R factor of 1.0×10^{-4}, $R = \Sigma[(\chi_M T)_{obs} - (\chi_M T)_{calc}]^2/\Sigma[(\chi_M T)_{obs}]^2$. In view of the slight discrepancy at very low temperature, an Hamiltonian introducing an axial zero field splitting term for Ni, $H = -J_{NiGd}(S_{Ni} \cdot S_{Gd}) + D_{Ni}S_z^2$, was also used. The fit, which is better, gives the following values: J_{NiGd} = 1.36 cm^{-1}, g = 2.07, D_{Ni} = 4.6 cm^{-1} with a R factor of 2.0×10^{-5} (Figure 3). In order to check the validity of these two sets of results, the MAGPACK program was used to fit the experimental magnetization curve at low temperature. As expected, the data set with a zero D value was not able to reproduce the experimental magnetization curve (Figure S5), particularly the region between 0.5–2 T, whereas a good agreement was obtained for the second data set (Figure 4). This result confirms the ferromagnetic Ni–Gd interaction and the presence of a zfs term for Ni.

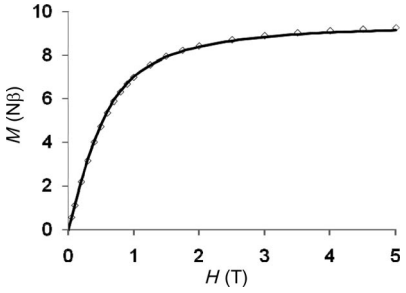

Figure 4. Field dependence of the magnetization for **4** at 2 K. The solid line corresponds to the best fit described in the text with J_{NiGd} = 1.36 cm^{-1}, D_{Ni} = 4.6 cm^{-1} and g = 2.07.

In the case of the isostructural Ni–Y complex **3**, which corresponds to an isolated Ni ion, the $\chi_M T$ product, equal to 1.22 $cm^3 mol^{-1}$ K at 300 K, remains constant until 15 K before decreasing to 0.87 $cm^3 mol^{-1}$ K at 2 K. The best fit yields a D_{Ni} value of 3.9 cm^{-1} with g = 2.22 and an R factor of 1.2×10^{-4} (Figure S6). These parameters reproduce the experimental M vs. H curve for complex **3** perfectly (Figure 5). Figure 5 confirms that it is not possible to fit the magnetization data for **3** without a zfs term D_{Ni} (dotted line).

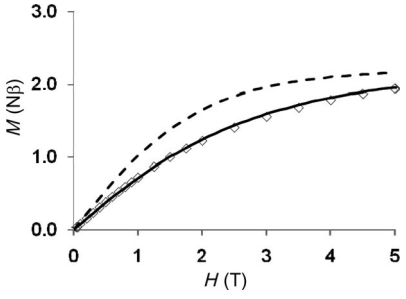

Figure 5. Field dependence of the magnetization for complex **3** at 2 K. The solid line corresponds to the best fit with D_{Ni} = 3.9 cm^{-1} and g = 2.22, while the dotted line corresponds to D_{Ni} = 0 and g = 2.22.

The variation of the $\chi_M T$ products against temperature for **1** and **2** is shown in Figure 6. $\chi_M T$ for the Ni–La complex **1**, which is constant and equal to 1.21 $cm^3 mol^{-1}$ K from 300 to 30 K, decreases to 0.68 $cm^3 mol^{-1}$ K at 2 K. For the Ni–Pr complex **2**, $\chi_M T$ starts at 2.70 $cm^3 mol^{-1}$ K at 300 K, is 2.61 $cm^3 mol^{-1}$ K at 100 K and decreases to reach 0.93 $cm^3 mol^{-1}$ K at 2 K. The Pr ion possesses an orbital contribution with strong spin–orbit coupling responsible for the decrease in $\chi_M T$ as T decreases. In the presence of orbital degeneracy, we have no general solution to deduce

the strength of the interaction parameter. Unfortunately, the empirical approach we investigated previously[16] does not allow qualitative information to be obtained for the two magnetic phenomena still active in the $\chi_M T$(**2**) – $\chi_M T$(**1**) difference curve, namely the Pr orbital contribution and the hypothetical Ni–Pr interaction. On the contrary, $\chi_M T$ for **1** indicates that zero field splitting is present. The best fit (Figure S7) gives a D_{Ni} parameter of 4.8 cm^{-1} with g = 2.18 and $R = 1 \times 10^{-4}$.

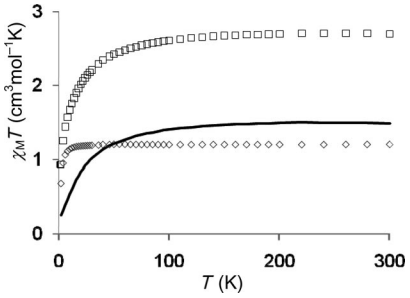

Figure 6. Experimental $\chi_M T$ vs. T for **1** (diamonds) and for **2** (squares). The solid line corresponds to the $\chi_M T$(**2**) – $\chi_M T$(**1**) difference.

Discussion

In view of the structure determinations, it does not seem possible to synthesize an isostructural Ni–Ln series where Ln varies from the lighter to the heavier Ln ions with use of *ortho*-vanillinato ligands in place of Schiff base ligands. The first reason for this observation comes from the presence of two independent ligands instead of a more rigid and unique Schiff base, and the choice of solvent has to be considered. We can also propose the effect of the size of the Ln ions as a reason. Our structural data show that on going from Pr to Y we introduce a deformation of the corresponding molecule that can be attributed, at least partially, to the ionic radius reduction. We also have to remember the way these molecules are built; starting with a monomeric nickel complex with two ovan ligands in a *trans* arrangement, the introduction of the Ln ion implies rotation of one ovan ligand and the breaking of a Ni–O bond in order to create the outer O_2O_2 coordination site able to accept the Ln ion. We have previously shown that nitrato ligands are chelated strongly to the Ln ions in acetone, whereas protic solvents such as methanol induce the formation of the $Ln(NO_3)^{2+}$ species.[17] These low-coordinated species can interact with two $Ni(ovan)_2$ units before their configuration change, which would explain the replacement of a nitrato ligand by an *ortho*-vanillinato ligand during the *trans* to *cis* conformation change of the $Ni(ovan)_2$ units, as a result of a chelating competition between these two ligands. On the contrary, we can imagine that the chelation of the three NO_3 ligands around the Ln ion in acetone impedes such competition.

Introduction of a chelating ovan ligand in the coordination sphere of the Ln ions in place of other anionic species was first observed in a Dy–Dy complex.[18] Since then, a similar replacement has been observed in a Cu–Tb complex,[6] and this work has given rise to a new example. It is worth noting that only one ovan ligand is added in each case, whereas two ligands enter into Ln coordination when diketone ligands are used.[19]

We have previously shown in Cu–Gd complexes that a correlation between the interaction parameter J and the dihedral angle defined as the angle between the OCuO and OGdO planes of the CuO_2Gd core does exist.[20] Reducing the bending of the CuO_2Gd core causes an increase in the ferromagnetic interaction. For Ni–Gd complexes, the largest J value published to date is 3.6 cm^{-1} and is associated with a dihedral angle of 4.2(5)°.[13] The J value obtained for **4** does not seem to agree with our previous data – a J value around or larger than 3.6 cm^{-1} is expected. A closer look at the molecular structure of **3** shows the main difference: the central NiO_2Gd core is the only part of the structure to be planar, the two independent, deprotonated *ortho*-vanillin ligands linked to the Ni and Gd ions depart from planarity to a large extent. This situation is different from the previous example,[13] where the Ni and Gd ions are coordinated to a unique ligand and the deformations are located at the NiO_2Gd core, as in the Cu–Gd complexes.[20] It becomes clear that the dihedral angle is not the correct parameter to gauge the interaction value. However, this supplementary degree of freedom induced by the two independent equatorial ligands in comparison to a more rigid and unique tetradentate ligand must be responsible for the slight decrease in the interaction parameter J.

Although the structure determination of complex **3** confirms that the dinuclear Ni–Y units are linked by hydrogen bonds to form a 1D chain, the isomorphous Ni–Gd complex can be treated from a magnetic point of view as isolated dinuclear units. Indeed, these hydrogen bonds involve the free and coordinated water molecules and the bridging nitrato ligand, which is known to be unable to support any significant magnetic interaction.[21] The good quality of the fit corroborates this hypothesis. A point that deserves more attention is the axial zfs term D, whose occurrence necessitates a departure from perfect octahedral environment for the Ni ion. The parameters given by the SHAPE program [S(Oh) = 0.63 for **2** and 0.14 for **3**] indicate that the Ni ions are not far from a perfect octahedral environment characterized by S(Oh) = 0. In comparison to the equatorial bond lengths, the two axial bond lengths are slightly longer by 0.070 Å in **2**; the difference is even smaller in **3** (0.074 and 0.034 Å). We must keep in mind that the six oxygen atoms surrounding the Ni ion differ in their nature: aldehyde, water molecules, deprotonated phenol and nitrato oxygen atoms are present. Furthermore, the three deprotonated oxygen atoms are positioned on the vertices of the same face of the octahedron; the vertices of the other face are occupied by neutral oxygen atoms in the case of **3**. Nevertheless, the homogeneity of D values found from the fitting of the magnetic data for **1**, **3** and **4** varies from 3.9 to 4.8 cm^{-1} and agrees with a D_{Ni} zfs term. Ni is the only magnetically active species in **1** and **3**. This assertion is con-

firmed by the observation of fine structure in the X-band EPR spectrum of **4** (Figure S8); the non-Kramer Ni ions in complexes **1** and **3** are unable to give an EPR spectrum.

Conclusions

This work demonstrates that simple, commercial *ortho*-vanillin ligands are able to yield interesting heterodinuclear Ni–Ln complexes. The nature and structure of these complexes appears to be greatly dependent on the solvent used during the synthesis. A ferromagnetic interaction is active in the Ni–Gd complex but in view of the isostructural Ni–Y entity, which presents a planar NiO_2Y core, the interaction ($1.36\ cm^{-1}$) is lower than that in a previously described Schiff base Ni–Gd complex ($3.6\ cm^{-1}$).[13] We conclude that the orbitals of the bridging phenoxo oxygen atoms are not correctly oriented to yield a large interaction, as a result of the departure from planarity in the equatorial plane introduced by the two independent ligands. Unfortunately, we do not have enough data to determine the presence and the nature of the interaction in the Ni–Pr complex qualitatively. Although minute geometrical deviations to a perfect octahedral environment are observed in these complexes, a zfs term based on the Ni ion is present and magnetically active, as confirmed by the occurrence of a fine structure in the X-band EPR spectrum of **4**.

Experimental Section

Materials: The metal salts, $Ni(CH_3COO)_2{\cdot}4H_2O$, $La(NO_3)_3{\cdot}6H_2O$, $Pr(NO_3)_3{\cdot}6H_2O$, $Gd(NO_3)_3{\cdot}6H_2O$, $Y(NO_3)_3{\cdot}6H_2O$ and *ortho*-vanillin (Aldrich) were used as purchased. High-grade solvents were used for preparing the complexes.

$(ovan)_2Ni(H_2O)_2$: $Ni(CH_3COO)_2{\cdot}4H_2O$ (1.25 g, 0.5×10^{-2} mol) was added to a stirred solution of *ortho*-vanillin (1.52 g, 1×10^{-2} mol) in methanol (60 mL), followed by addition of triethylamine (1 g, 1×10^{-2} mol). The mixture was heated for 30 min and then cooled to yielding a green precipitate, which was collected by filtration and dried. Yield: 1 g (50%). $C_{16}H_{18}NiO_8$ (397.0): calcd. C 48.4, H 4.5; found C 48.0, H 4.3.

$[(H_2O)_2Ni(ovan)_2La(NO_3)_3]$ (1) and $[(H_2O)_2Ni(ovan)_2Pr(NO_3)_3]$ (2): Addition of $La(NO_3)_3{\cdot}6H_2O$ (0.43 g, 1 mmol) or $Pr(NO_3)_3{\cdot}6H_2O$ (0.43 g, 1 mmol) to a stirred suspension of $(ovan)_2Ni(H_2O)_2$ (0.4 g, 1 mmol) in acetone (10 mL) induced dissolution of the nickel complex. The mixture was heated for 15 min, and the cold solution was then filtered and concentrated to half of the original volume. Slow evaporation yielded powder for **1** and crystals suitable for XRD for **2**, which were isolated by filtration and dried. Yield: 0.60 g (82%) for **1** and 0.47 g (65%) for **2**. $C_{16}H_{18}LaN_3NiO_{17}$ (721.9): calcd. C 26.6, H 2.5, N 5.8; found C 26.2, H 2.4, N 5.4. IR (KBr): $\tilde{\nu}$ = 3385 (m), 1621 (s), 1609 (m), 1551 (m), 1466 (m), 1447 (s), 1418 (s), 1300 (s), 1238 (m), 1209 (s), 1167 (w), 1100 (w), 1066 (w), 1035 (w), 947 (m), 852 (w), 818 (w), 782 (w), 730 (m), 649 cm^{-1}. $C_{16}H_{18}N_3NiO_{17}Pr$ (723.9): calcd. C 26.6, H 2.5, N 5.8; found C 26.4, H 2.4, N 5.3. IR (KBr): $\tilde{\nu}$ = 3434 (m), 1624 (s), 1608 (m), 1552 (m), 1467 (m), 1447 (s), 1437 (s), 1415 (s), 1295 (s), 1274 (m), 1237 (m), 1205 (s), 1170 (w), 1094 (w), 1064 (w), 1038 (w), 946 (m), 853 (w), 814 (w), 783 (w), 728 (m), 648 cm^{-1}.

$[(H_2O)Ni(ovan)_2(\mu\text{-}NO_3)Y(ovan)(NO_3)_2]H_2O$ (3) and $[(MeOH)Ni(ovan)_2(\mu\text{-}NO_3)Gd(ovan)(NO_3)_2]$ (4): A mixture of $(ovan)_2Ni(H_2O)_2$ (0.4 g, 1 mmol) and $Gd(NO_3)_3{\cdot}6H_2O$ (0.45 g, 1 mmol) or $Y(NO_3)_3{\cdot}6H_2O$ (0.38 g, 1 mmol) in methanol (10 mL) was heated and stirred for 20 min to yield a green solution, which was filtered after cooling and concentrated to half of the original volume. Addition of isopropyl alcohol (5 mL) and slow evaporation yielded a precipitate for **3** and crystals suitable for XRD in the case of **4**, which were isolated by filtration and dried. Yield: 0.33 g (40%) for **3** and 0.22 g (30%) for **4**. $C_{24}H_{25}N_2NiO_{17}Y$ (761.1): calcd. C 37.9, H 3.3, N 3.7; found C 37.5, H 3.1, N 3.4. IR (KBr): $\tilde{\nu}$ = 3408 (m), 1628 (s), 1609 (m), 1546 (m), 1474 (m), 1451 (m), 1431 (m), 1406 (s), 1299 (s), 1246 (m), 1208 (s), 1170 (w), 1093 (w), 1066 (w), 1056 (w), 1031 (w), 949 (m), 859 (w), 810 (w), 782 (w), 743 (w), 728 (m), 650 cm^{-1}. $C_{25}H_{25}GdN_2NiO_{16}$ (825.4): calcd. C 36.4, H 3.0, N 3.4; found C 36.0, H 2.7, N 3.2. IR (KBr): $\tilde{\nu}$ = 3412 (m), 1629 (s), 1609 (m), 1551 (m), 1545 (m), 1473 (m), 1452 (m), 1430 (m), 1406 (s), 1308 (m), 1294 (m), 1245 (m), 1208 (s), 1169 (w), 1093 (w), 1066 (w), 1055 (w), 1029 (w), 949 (m), 858 (w), 811 (w), 782 (w), 743 (w), 729 (m), 650 cm^{-1}.

Physical Measurements: Elemental analyses were carried out at the Laboratoire de Chimie de Coordination Microanalytical Laboratory in Toulouse, France, for C, H, and N. IR spectra were recorded with a Spectrum 100 FTIR Perkin–Elmer spectrophotometer by using the ATR mode. Magnetic data were obtained with a Quantum Design MPMS SQUID susceptometer. Magnetic susceptibility measurements were performed in the 2–300 K temperature range in a 0.1 T applied magnetic field, and diamagnetic corrections were applied by using Pascal's constants.[22] Isothermal magnetization measurements were performed up to 5 T at 2 K. The magnetic susceptibilities have been computed by exact calculations of the energy levels associated to the spin Hamiltonian through diagonalization of the full-matrix with a general program for axial and rhombic symmetries,[23] and the magnetizations with the MAGPACK program package.[24] Least-squares fittings were accomplished with an adapted version of the function-minimization program MINUIT.[25]

Crystallographic Data Collections and Structure Determinations for 2 and 3: Crystals of **2** and **3** were kept in their mother liquor until they were dipped into oil. The crystals were mounted on a Mitegen micromount and quickly cooled to 180 K. The selected crystals of **2** (green, $0.5\times0.45\times0.45$ mm) and **3** (yellow green, $0.125\times0.1\times0.1$ mm) were mounted on an Enraf–Nonius CAD4 or a Xcalibur Oxford Diffraction diffractometer by using graphite-monochromated Mo-K_α radiation (λ = 0.71073 Å) and equipped with an Oxford Instrument Cooler Device. Data were collected at room temperature for **2** and at low temperature (180 K) for **3**. The final unit cell parameters were obtained by least-squares refinements. The structures were solved by direct methods by using SHELXS97[26] or SIR92,[27] and refined by least-squares procedures on F^2 with the program SHELXL97[26] included in the software package WinGX version 1.63.[28] Positional parameters of the H atoms of water molecules in **2** were obtained from difference Fourier syntheses and verified by the geometric parameters of the corresponding hydrogen bonds. The atomic scattering factors were taken from international tables for X-ray crystallography.[29] All non-hydrogen atoms were anisotropically refined, and in the last cycles of refinement, a weighting scheme was used, where weights are calculated from the following formula: $w = 1/[\sigma^2(F_o^2) + (aP)^2 + bP]$ where $P = (F_o^2 + 2F_c^2)/3$. Drawings of molecules were produced with the programs ZORTEP[30] and ORTEP32 with 30% probability displacement ellipsoids for non-hydrogen atoms.[31] CCDC-763005 (for **2**) and -763006 (for **3**) contain the supplemen-

tary crystallographic data for this paper. These data can be obtained free of charge from The Cambridge Crystallographic Data Centre via www.ccdc.cam.ac.uk/data_request/cif.

Supporting Information (see footnote on the first page of this article): Powder XRD pattern for **4**, structures showing the hydrogen bonds in complexes **2** and **3**, temperature dependence of the $\chi_M T$ products for **4**, **3**, **1** and field dependence of magnetization for **4** are presented.

Acknowledgments

This work was supported by the European Union sixth framework program NMP3-CT-2005-515767 entitled "MAGMANet: Molecular Approach to Nanomagnets and Multifunctional Materials". The authors are grateful to Dr. A. Mari for technical assistance.

[1] C. Benelli, D. Gatteschi, *Chem. Rev.* **2002**, *102*, 2369–2387.
[2] M. Sakamoto, K. Manseki, H. Okawa, *Coord. Chem. Rev.* **2001**, *219–221*, 379–414.
[3] R. Gheorghe, P. Cucos, M. Andruh, J. P. Costes, B. Donnadieu, S. Shova, *Chem. Eur. J.* **2006**, *12*, 187–203.
[4] J. P. Costes, F. Dahan, A. Dupuis, J. P. Laurent, *Inorg. Chem.* **1997**, *36*, 3429–3433.
[5] J. P. Costes, F. Dahan, A. Dupuis, J. P. Laurent, *C R. Acad. Sci. Paris, IIc* **1998**, 417–420.
[6] T. Kajiwara, M. Nakano, S. Takaishi, M. Yamashita, *Inorg. Chem.* **2008**, *47*, 8604–8606.
[7] J. P. Costes, F. Dahan, F. Nicodème, *Inorg. Chem.* **2001**, *40*, 5285–5287.
[8] J. Tang, I. Hewitt, N. T. Madhu, G. Chastanet, W. Wernsdorfer, C. E. Anson, C. Benelli, R. Sessoli, A. K. Powell, *Angew. Chem. Int. Ed.* **2006**, *45*, 1729–1734.
[9] Y. Z. Zheng, Y. Lan, C. E. Anson, A. K. Powell, *Inorg. Chem.* **2008**, *47*, 10813–10815.
[10] P. H. Lin, T. J. Burchell, L. Ungur, L. F. Chibotaru, W. Wernsdorfer, M. Murugesu, *Angew. Chem. Int. Ed.* **2009**, *48*, 9489–9492.
[11] J. M. Stewart, E. C. Lingafelter, J. D. Breazeale, *Acta Crystallogr.* **1964**, *17*, 1481–1490.
[12] J. P. Costes, F. Dahan, J. P. Laurent, *Inorg. Chem.* **1994**, *33*, 2738–2742.
[13] J. P. Costes, F. Dahan, A. Dupuis, J. P. Laurent, *Inorg. Chem.* **1997**, *36*, 4284–4286.
[14] M. C. Etter, *Acc. Chem. Res.* **1990**, *23*, 120–126.
[15] S. Alvarez, D. Avnir, M. Llunell, M. Pinsky, *New J. Chem.* **2002**, *26*, 996–1009.
[16] J. P. Costes, F. Dahan, A. Dupuis, J. P. Laurent, *Chem. Eur. J.* **1998**, *4*, 1616–1620.
[17] J. P. Costes, J. García-Tojal, J. P. Tuchagues, L. Vendier, *Eur. J. Inorg. Chem.* **2009**, 3801–3806.
[18] J. P. Costes, F. Dahan, F. Nicodème, *Inorg. Chem.* **2003**, *42*, 6556–6563.
[19] J. P. Costes, F. Dahan, W. Wernsdorfer, *Inorg. Chem.* **2006**, *45*, 5–7.
[20] J. P. Costes, F. Dahan, A. Dupuis, *Inorg. Chem.* **2000**, *39*, 165–168.
[21] H. M. J. Hendricks, P. J. M. Birker, J. van Rijn, G. C. Verschoor, J. Reedijk, *J. Am. Chem. Soc.* **1982**, *104*, 3607–3617.
[22] P. Pascal, *Ann. Chim. Phys.* **1910**, *19*, 5–70.
[23] A. K. Boudalis, J.-M. Clemente-Juan, F. Dahan, J.-P. Tuchagues, *Inorg. Chem.* **2004**, *43*, 1574–1586.
[24] J. J. Borrás-Almenar, J. M. Clemente-Juan, E. Coronado, B. S. Tsukerblat, *Inorg. Chem.* **1999**, *38*, 6081–6088; J. J. Borrás-Almenar, J. M. Clemente-Juan, E. Coronado, B. S. Tsukerblat, *J. Comput. Chem.* **2001**, *22*, 985–991.
[25] *MINUIT Program, a System for Function Minimization and Analysis of the Parameters Errors and Correlations*: F. James, M. Roos, *Comput. Phys. Commun.* **1975**, *10*, 343–367.
[26] G. M. Sheldrick, *SHELX97 (includes SHELXS97, SHELXL97, CIFTAB) – Programs for Crystal Structure Analysis (Release 97-2)*, Institut für Anorganische Chemie der Universität, Göttingen, Germany, **1998**.
[27] *SIR92 – A Program for Crystal Structure Solution*: A. Altomare, G. Cascarano, C. Giacovazzo, A. Guagliardi, *J. Appl. Crystallogr.* **1993**, *26*, 343–350.
[28] *WINGX – 1.63 Integrated System of Windows Programs for the Solution, Refinement and Analysis of Single Crystal X-ray Diffraction Data*: L. Farrugia, *J. Appl. Crystallogr.* **1999**, *32*, 837–838.
[29] *International Tables for X-ray Crystallography*, Kynoch Press, Birmingham, England, **1974**, vol. IV.
[30] L. Zsolnai, *ZORTEP – Program for Molecular Graphics*, University of Heidelberg, Heidelberg, Germany, **1996**.
[31] *ORTEP32 for Windows*: L. Farrugia, *J. Appl. Crystallogr.* **1997**, *30*, 565–568.

Received: January 27, 2010
Published Online: April 30, 2010

